Chapter 5: **CRYSTAL GROWTH OF RTP:(Nb,Ln) SINGLE CRYSTALS**

Crystals are appreciated both for their appearance and their unique physical properties, which by the photonic industry uses in appliances that we come across every day. Single crystals, crystalline layers and multilayer structures are today playing an increasingly important role in technology.

At the beginning of the 20th century, crystal growth was still a curiosity. However, knowledge of crystal structures and the relationship between chemical bonds and the physical properties, and the introduction of various crystal growth techniques, led to the emergence of many new compounds. However, the complexity of crystal-growth processes, and their high sensitivity to tiny fluctuations, make reproducibility difficult. For this reason crystal growth cannot be viewed simply as a science: it is also an art.[197]

5.1. Crystal Growth.

We grew RTP, RTP:Nb and RTP:(Nb,Ln) crystals with Ln = Er or Yb in self-fluxes and in fluxes containing WO_3 by the Top-Seeded Solution Growth technique and slow-cooling of the solution. The experiments lasted between 2 and 4 weeks on average. We prepared the growth solutions by mixing the desired amount of Rb_2CO_3, $NH_4H_2PO_4$, TiO_2, Nb_2O_5, Er_2O_3, Yb_2O_3 and WO_3 (p.a.), used as initial reagents. In these experiments we used two types of Pt crucibles. One was a conical crucible of 25 cm^3 filled with solutions weighing around 25-45 g and the other was a cylindrical crucible of 125 cm^3 filled with solutions weighing around 160 g. Descriptions of the methods for preparing the solutions can be found in all papers included in this Thesis. When the growth run was completed, the crystal was lifted 5 mm upwards from the surface of the solution and cooled to room temperature at a rate of 15-50 $K \cdot h^{-1}$ to avoid thermal stresses.

The conditions and the results in crystal-growth experiments are very dispersed among all the papers included in this Thesis. To make it easier to understand these results, therefore, we have grouped them all together in this section. We used several systems to fix the crystal seeds. These techniques form the structure of this chapter.

5.1.1. Crystal growth without additional stirring.

In our first experiments on crystal growth, we used only the normal stirring produced by the rotation of the growing crystal, i.e. we did not use any other element to stir the solution. To prevent inclusion flaws from forming during the advanced stages of growth, it is important to rotate the seed and allow sufficient circulation of the flux.[183] We obtained the first seeds from growth experiments by spontaneous nucleation on the surface of the solution. We then oriented the crystal and cut slices parallel to the ***b*** and ***c*** crystallographic direction to be used as seeds for the TSSG experiments. We used crystal seeds of RTP, laced at the end of an alumina rod and placed away from the centre of the surface of the solution with the ***b*** or ***c*** direction, depending on the crystal growth experiment, normal to the surface of the solution. In all cases the ***a*** crystallographic direction was placed on the radial direction of the rotation movement. These crystal seeds had typical dimensions of 1.5 × 5.0 × 1.5 mm in the ***a*** × ***b*** × ***c*** directions when the crystals were grown in ***b***-oriented seeds, and 1.5 × 1.5 × 5.0 mm when the crystals were grown in ***c***-oriented seeds. We made a small groove on the (010) or (001) face of the crystal seed, depending on the experiment (if the crystal seed was ***c***-oriented we made the groove in the (010) face and if the crystal seed was ***b*** oriented we made the groove in the (001) face). This enabled us to lace the crystal seed to the alumina rod using thin Pt wire. We determined the saturation temperature (T_s) by observing the growth or dissolution of the crystal seed in contact with the solution.

When there was no crystal growth or when dissolution was low, this was taken as the T_s. The crystal seed was rotated at an angular speed of 45 rpm and the direction of the rotation was changed every 50 s. This system was chosen because it proved successful in the crystal growth of KTP and derivative crystals,[198] and because it introduces additional other flows in the solution to those of a thermal convective origin, which improves its homogeneity. With this system we successfully grew single crystals of RTP in self-flux and in fluxes containing 10 and 20 mol % of WO_3. Table 5.1 shows the most significant results from these experiments.

Table 5.1. *Growth data associated with RTP, RTP:W, RTP:(Nb,Er), RTP:(Nb,Er,W) and RTP:(Nb,Yb) single crystals grown on a crystal seed placed (centred or not-centred) on the surface of the solution.*

A	B	C	D	E	F	G	H	I
42.0-28.0-30.0-0.0-0.0-0.0-0.0	152	1204	***c***	NC	2 K/0.1K·h^{-1} 2 K/0.05 K·h^{-1} 9.5 K/0.02K·h^{-1}	6.3 × 12.2 × 7.7	1.054	Very good
42.0-28.0-30.0-0.0-0.0-0.0-0.0	152	1206	***b***	NC	2 K/0.1K·h^{-1} 2 K/0.05 K·h^{-1} 5.5 K/0.02K·h^{-1}	5.0 × 8.0 × 13.0	0.919	Very good
42.0-28.0-30.0-0.0-0.0-0.0-0.0	152	1204	***b***	NC	2.2 K/0.1K·h^{-1} 2 K/0.05 K·h^{-1} 10.0 K/0.02K·h^{-1}	8.5 × 9.2 × 18.0	1.928	Very good
42.0-28.0-28.5-0.6-0.9-0.0-0.0	164	1190	***b***	NC	2 K/0.1K·h^{-1} 2 K/0.05 K·h^{-1} 12.5 K/0.02K·h^{-1}	3.0 × 17.5 × 6.0	0.676	Small cracks
42.0-28.0-27.9-1.2-0.9-0.0-0.0	169	1187	***b***	NC	2 K/0.1K·h^{-1} 5 K/0.05 K·h^{-1} 15 K/0.03K·h^{-1}	3.5 × 17.0 × 8.0	0.809	Cracks
43.9-23.6-22.5-0.0-0.0-0.0-10.0	31	1158	***c***	C	20.5 K/0.1K·h^{-1}	5.9 × 11.4 × 6.5	0.788	Very good
43.9-23.6-22.5-0.0-0.0-0.0-10.0	32		***c***	C	40 K/0.1K·h^{-1}	8.5 × 14.6 × 5.8	1.645	Inclusions
44.2-19.0-16.8-0.0-0.0-0.0-20.0	43	1152	***b***	C	28.9 K/0.1K·h^{-1}	6.5 × 8.1 × 16.4	1.301	Very good
44.2-19.0-16.8-0.0-0.0-0.0-20.0	43	1147	***c***	C	30.0 K/0.1K·h^{-1}	8.7 × 12.2 × 9.3	1.478	Small inclusions
44.2-19.0-16.8-0.0-0.0-0.0-20.0	43	1161	***c***	C	30.0 K/0.1K·h^{-1}	7.4 × 6.2 × 15.0	1.170	Very good
43.7-23.5-12.8-0.0-0.0-0.0-20.0	35	1141	***c***	C	25.5 K/0.1K·h^{-1}	11.0 × 5.5 × 6.0	0.562	Very good
43.7-23.5-12.8-0.0-0.0-0.0-20.0	35	1137	***b***	C	20.0 K/0.1K·h^{-1}	6.5 × 2.6 × 7.0	0.141	Small inclusions
42.0-28.0-27.9-1.2-0.9-0.0-0.0	30	1182	***b***	NC	2 K/0.2K·h^{-1} 13.5 K/0.1 K·h^{-1} 5 K/0.05K·h^{-1}	1.8 × 1.7 × 3.5	0.019	Very good
42.0-28.0-27.9-1.2-0.9-0.0-0.0	30	1181	***b***	NC	20 K/0.2K·h^{-1} 13.3 K/0.1 K·h^{-1}	2.5 × 5.5 × 16.0	0.422	Inclusions and cracks
42.0-28.0-28.2-0.9-0.0-0.9-0.0	31	1188	***b***	NC	10 K/0.2K·h^{-1} 19 K/0.1 K·h^{-1}	2.6 × 6.2 × 21.4	0.600	Inclusions and cracks
41.7-24.5-22.6-0.7-0.5-0.0-10.0	15	1196	***c***	C	15 K/0.1K·h^{-1}	2.1 × 6.4 × 3.6	0.092	Cracks
44.2-19.0-16.0-0.5-0.3-0.0-20.0	24	1132	***c***	C	32 K/0.1K·h^{-1}	2.6 × 9.2 × 5.9	0.295	Cracks

A: Solution composition (Rb_2O-P_2O_5-TiO_2-Nb_2O_5-Er_2O_3-Yb_2O_3-WO_3) (mol %). **B**: Solution weight (g). **C**: T_s (K). **D**: Seed crystallographic orientation. **E**: Seed position, centred (C) or non-centred (NC). **F**: Cooling program. **G**: Crystal dimensions in ***a***, ***b*** and ***c*** crystallographic directions, respectively (mm). **H**: Crystal weight (g). **I**: Quality of the crystal.

In the experiments performed in Pt crucibles of 125 cm^3, we can see that for RTP, when the cooling program is carried out more slowly in a similar range of temperatures, the crystal obtained is larger. It seems that the process incorporating structural units to the crystal is more efficient when we apply a slow cooling program, because in viscous solutions, as it is our solution when we did not use WO_3, there exists a level of difficulty for the structural units to reach the crystal-solution interface. If we apply a slow cooling program we gives more time to the system to get conditions near those of the equilibrium.

In the experiments performed in Pt crucibles of 25 cm^3, there were significant differences between the growth conditions of RTP single crystals in self-fluxes and those in fluxes containing WO_3. In solutions containing WO_3, the time of homogenisation was shorter, the interval cooling of temperatures could be wider and the cooling process to obtain high quality crystals could be made faster than in self-fluxes. We also checked whether it was possible to obtain inclusion-free single crystals in a seed located at the centre of the surface of the solution. As reported in the literature,[185] we expected the solutions containing WO_3 to be less viscous than self-fluxes, thus allowing a better homogenisation of the solution by only natural convective fluxes due to the temperature gradient. In solutions containing 10 % of WO_3, we found that the wider the interval of cooling, the larger the crystal. However, some inclusions appeared in the lower part of the crystal, which was also redissolved, perhaps because the gradient of temperature in the crucible was not suitable. In solutions containing 20% of WO_3 we found that when the solution was richer in TiO_2 and Rb_2O_3 and poorer in P_2O_5, the temperature of saturation increased. In all cases, however, we obtained high-quality single crystals.

The crystal growth conditions did not change significantly when the orientation of the crystal seeds was different. The only difference was in the morphology of the crystals. These results show that the velocity of growth along the ***a***, ***b*** and ***c*** directions was similar, but that it was higher in the ***c*** direction when the crystals were grown on a ***b***-oriented seed, and higher in the ***b*** direction when the crystals were grown on a ***c***-oriented seed. In general we obtained very transparent single crystals that were large enough for later optical characterisations (see Figure 5.1). Figure 5.1 also shows a schematic drawing of the dominant faces of each crystal. We observed no change in the morphology of the crystals with or without W, which shows the typical {100}, {201}, $\{20\bar{1}\}$, {110}, {011} and $\{01\bar{1}\}$ forms of the RTP crystals (see Figure 6 in *paper V*). However, in crystals grown in solutions containing 20% of WO_3 and richer in P_2O_5, the {100} form of the crystals narrowed and tended to disappear. In Figure 5.1 (a), we can see the characteristic round mark often found on an as-grown (011) and (110) crystal surfaces. This was caused by a drop of flux sticking to the crystal surface after it was lifted out of the solution. This mark can also be seen in Figure 5.1 (b) in the (201) face of the crystal. Similar features have been reported for other crystals of the KTP family.[199]

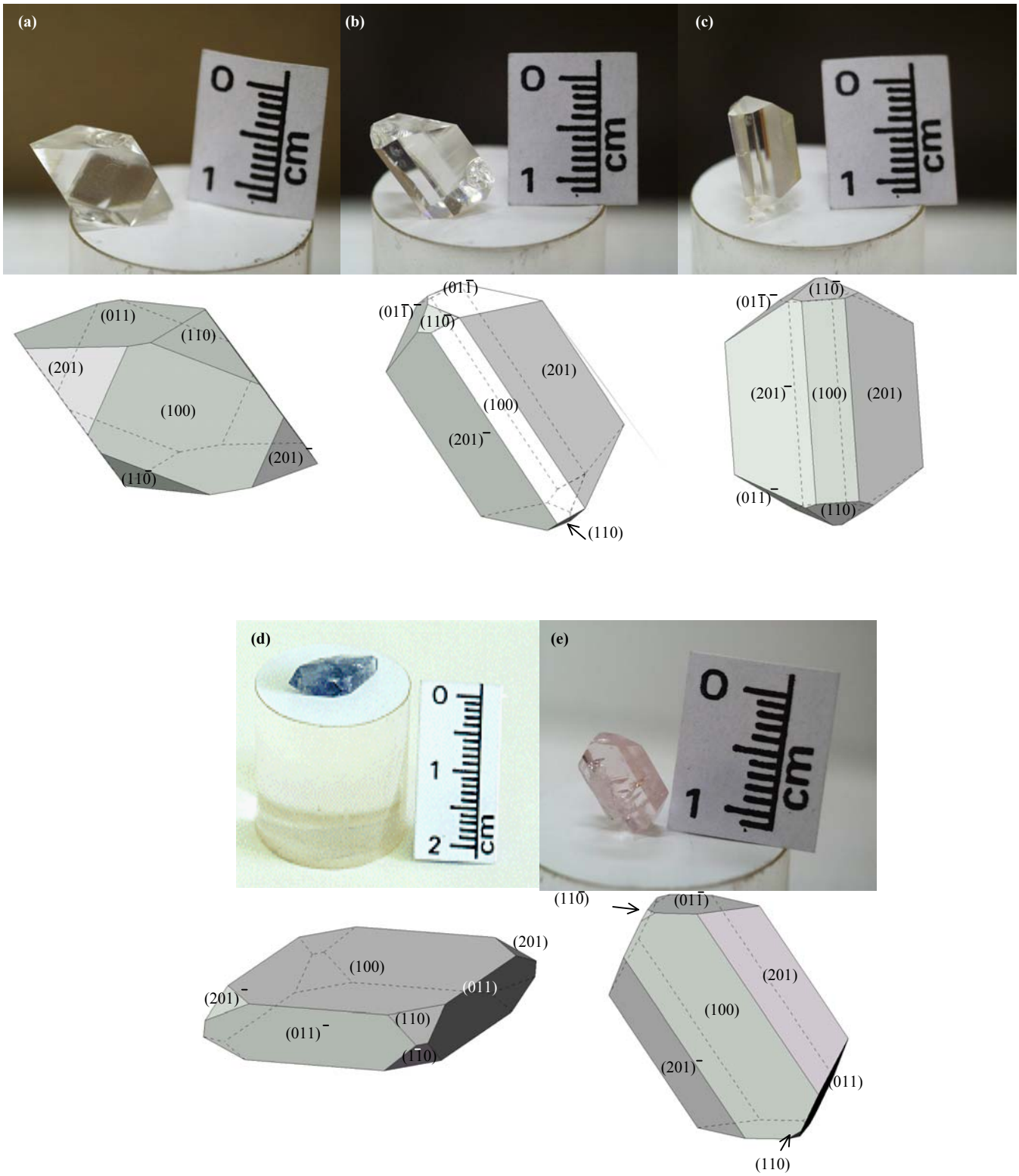

Figure 5.1. *Single crystals of (a)* ***b****-oriented RTP, (b)* ***c****-oriented RTP, (c)* ***c****-oriented RTP:W, (d)* ***b****-oriented RTP:(Nb,Er), and (e)* ***c****-oriented RTP:(Nb,Er,W) grown on a crystal seed placed (centred or non-centred) on the surface of the solution without additional stirring.*

We then grew single crystals of RTP:(Nb,Ln) (Ln = Er or Yb) in non-centred crystal seeds. In these experiments we increased the rotation velocity to 60-70 rpm because we saw that the solution was more viscous. To develop these experiments part of the TiO_2 of the solution was substituted by Nb_2O_5 + Er_2O_3 or Nb_2O_5 + Yb_2O_3. The different dopant concentrations we used are shown in Table 5.1. We used crystal seeds of RTP with the ***b*** crystallographic direction normal to the surface of the solution and the ***a*** direction again in the radial direction of the rotation movement.

In these solutions, and irrespective of the flux used, the average time of homogenisation increased and the average rate of growth of inclusion-free single crystals decreased as the concentration of niobium in the solution increased. Also, some cracks were seen to come from the crystal seed. However, when we used a slower cooling program, the quality of the crystals was better. In solutions containing W, the temperature of saturation of the crystals containing Nb and Er was clearly lower. Our results show that in general the dimension in the ***c*** direction was larger than the dimensions in the other directions and the dimension in the ***a*** direction was the smallest.

5.1.2. The change in morphology introduced by Nb.

As we can clearly see in Figures 5.1(d) and 5.1(e), the presence of Nb significantly changed the morphology of the crystals. We had not seen this change in morphology in the crystals of the KTP family doped only with Ln.[120]

The morphology of KTP crystals was first studied by Voronkova and Yanovskii[200] and Pavlova et al.[201] The crystal habit is built up of {100}, {201}, $\{20\bar{1}\}$, {011}, $\{01\bar{1}\}$, and {110} faces. The {201} and {011} planes form sharp caps along the ***c*** axis, whereas the {011} and {110} planes form less sharp caps along the ***b*** axis. The morphology is symmetrical. It resembles the *mmm* symmetry, which is higher than the internal structure (*mm2* symmetry) of KTP. Bolt and Bennema[202] made a periodic bond chain analysis of the structure of KTP and found that the morphological importance of the crystal forms of KTP is {100}>{201}>{011}>{110}.

RTP and RTP:(Nb,Ln) crystals grew with the same forms as KTP crystals, but RTP:(Nb,Ln) crystals grew as thin plates. The {100} face is more developed than the other faces of the crystal. As we found when determining the crystallisation region of RTP in fluxes containing Nb_2O_5 and Ln_2O_3, this change in morphology can be only attributed to the presence of Nb in the crystals. This agrees with the previous results for KTP:Nb crystals.[203] Figure 6 in *paper V* shows the morphologies of an RTP crystal and an RTP:(Nb,Er) crystal in a schematic view drawn with the Shape utility.[204]

Changes in the morphology of crystals grown in doped solutions can be caused by the growth sites on the crystal being poisoned by the attachment of dopant species. In fact, we found that the presence of Nb_2O_5 in the solution, even at low concentrations, affects the morphology of the crystals

and slows the crystal growth process. We observed, by SEM, macro-hillocks of growth in the {100} face of RTP:Nb crystals (see Figure 5.2). Figure 5.2 also shows a schematic view of the crystal to illustrate its faces and orientation. The edges of these hillocks are parallel to the [010], [011], and $[01\bar{1}]$ faces. The macro-steps are parallel to the [010] direction. These macro-hillocks were not observed in the {100} face of pure RTP crystals.

We tried to study these changes in the morphology of the crystals more fully using atomic force microscopy (AFM), but the high polarisability of the crystal made it difficult to do this. In general, the faces were dirty and it was therefore difficult to see anything. The results were best when the crystals were cleaned in an ultrasound bath for 5 minutes with a solution of 0.5 g of Na_2HPO_4 and 0.5 g of NaH_2PO_4 in 40 ml of water. In Figure 5.3 we show a hillock of growth in the (100) face of an RTP:Nb crystal. This figure was obtained by superimposing several AFM images. A general image of the crystal, taken with an optical microscope, is included. This shows with an A the area observed by AFM. The edges of this spiral are parallel to the same directions of the macro-hillock observed by SEM. The steps observed in this figure have a height of between 34 and 232 Å (see Figure 5.4). This corresponds, approximately to between 3 and 20 times the length of the parameter ***a***.

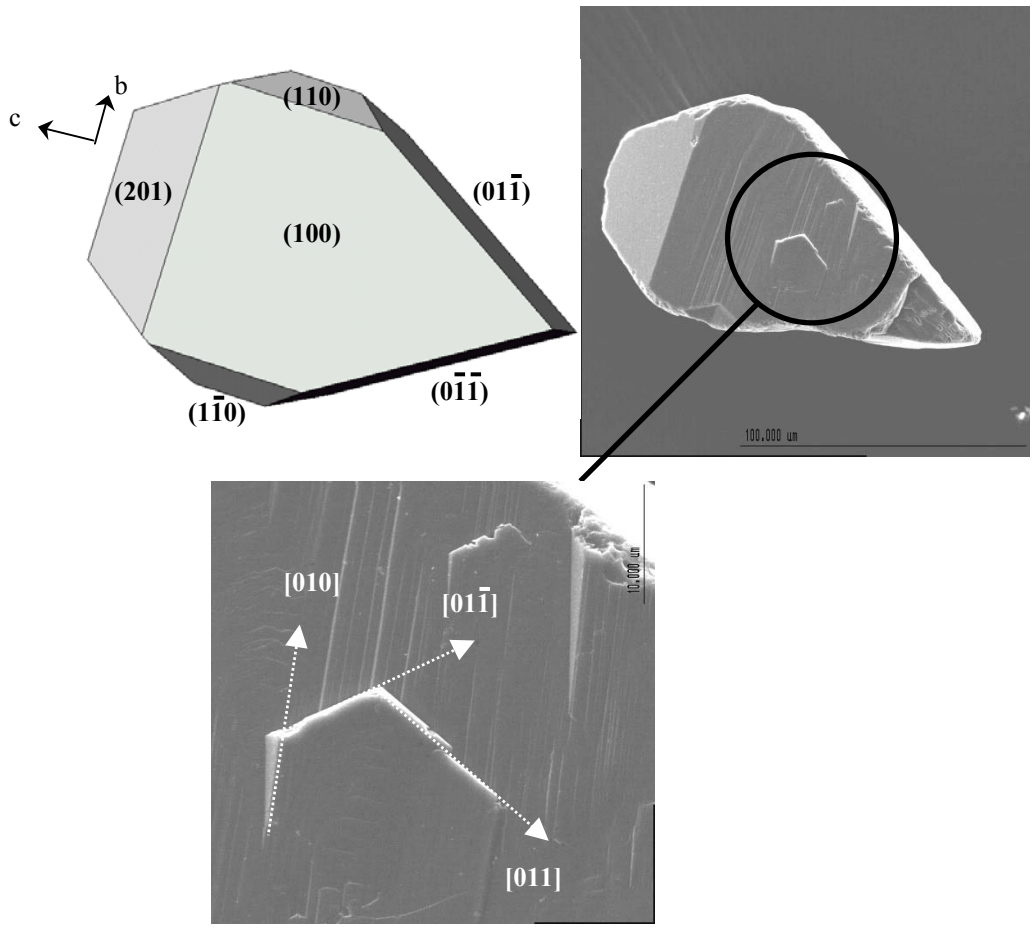

Figure 5.2. *Macro-hillock of growth on the (100) face of an RTP:Nb crystal. Images obtained by SEM.*

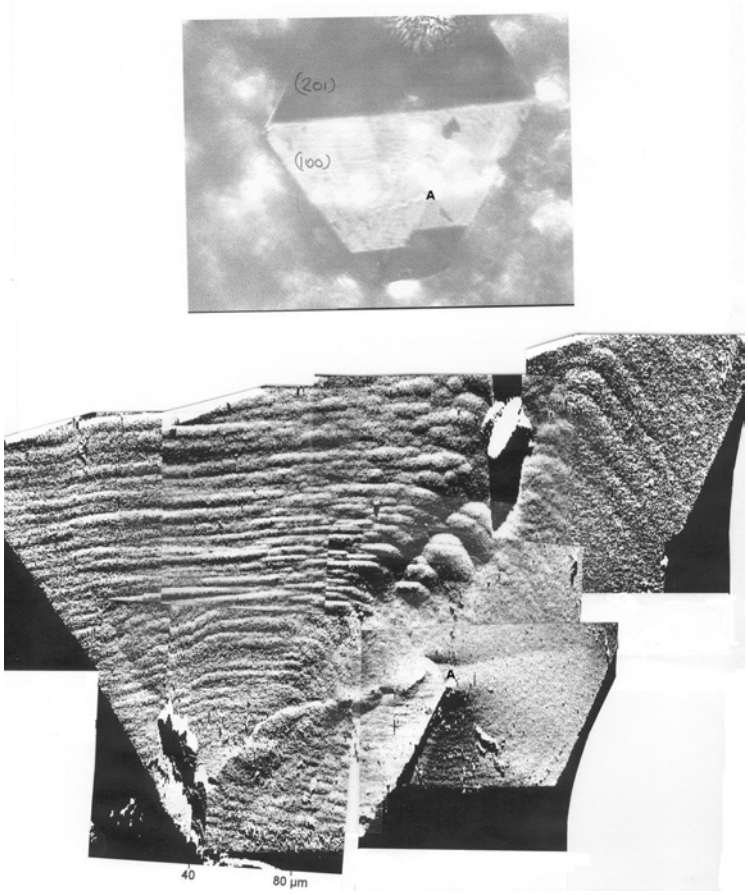

Figure 5.3. *Macro-hillock of growth in the (100) face of an RTP:Nb crystal.*

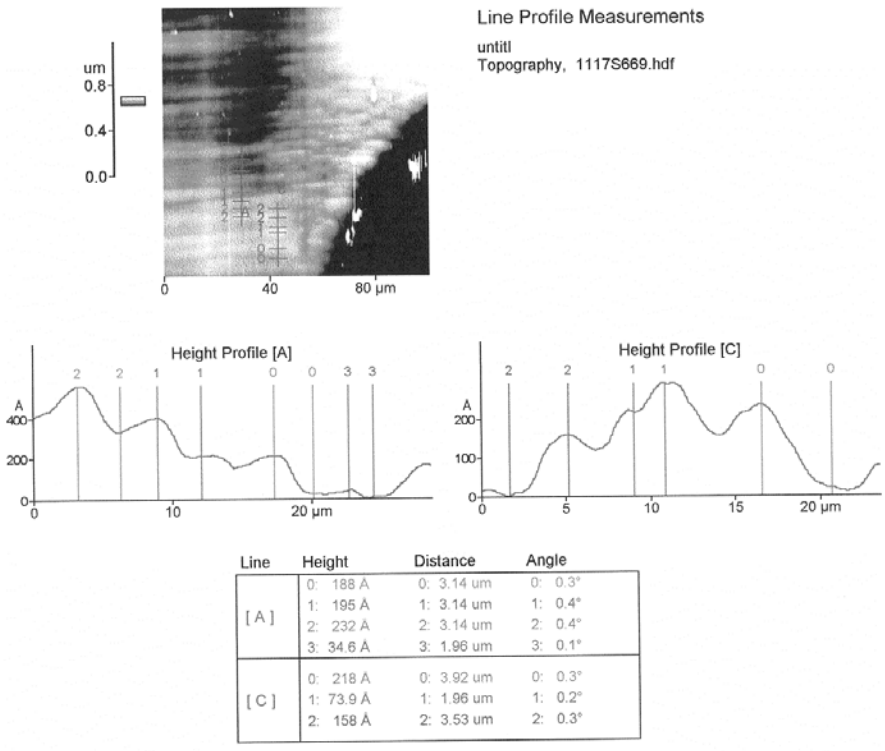

Line	Height	Distance	Angle
[A]	0: 188 Å	0: 3.14 um	0: 0.3°
	1: 195 Å	1: 3.14 um	1: 0.4°
	2: 232 Å	2: 3.14 um	2: 0.4°
	3: 34.6 Å	3: 1.96 um	3: 0.1°
[C]	0: 218 Å	0: 3.92 um	0: 0.3°
	1: 73.9 Å	1: 1.96 um	1: 0.2°
	2: 158 Å	2: 3.53 um	2: 0.3°

Figure 5.4. *Profile of the steps in the (100) face of an RTP:Nb crystal.*

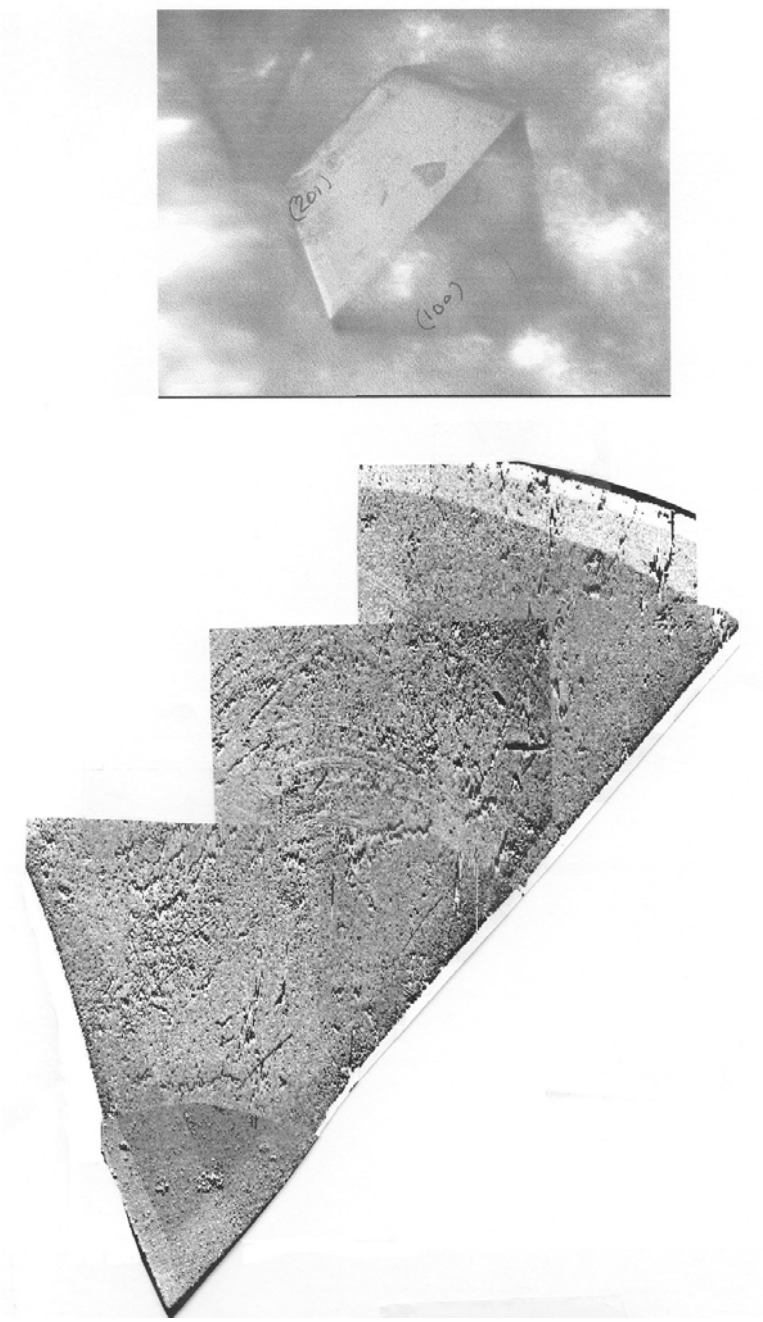

Figure 5.5. *AFM image of the (201) face of an RTP:Nb crystal*

Figure 5.5 shows a composition of several AFM images for the (201) face of an RTP:Nb crystal. The image was taken with the same crystal as in Figure 5.3. As we can see, this face is very flat and there were no steps. The other faces of the crystal did not provide any relevant information.

Clearly, therefore, the {100} face grows in a very different way to the {201} face. As we could not do a similar study observing both {100} and {201} faces of pure RTP crystals, we do not know whether this behaviour is common in this family of crystals. The only reference we have is the paper published by Bolt et al.[199] about KTP. If we compare their results with ours, we can see that in the {100} face they found large growth hillocks lying approximately at the centre of these faces with

growth steps orientated parallel to the ***b***-axis, but they did not, as we clearly did, find the other steps parallel to the [011] and $[01\bar{1}]$ directions. Nevertheless the steps they observed were lower than ours by 1 or 2 orders of magnitude. They observed growth hillocks in the {201} face, albeit with difficulty, but we could not.

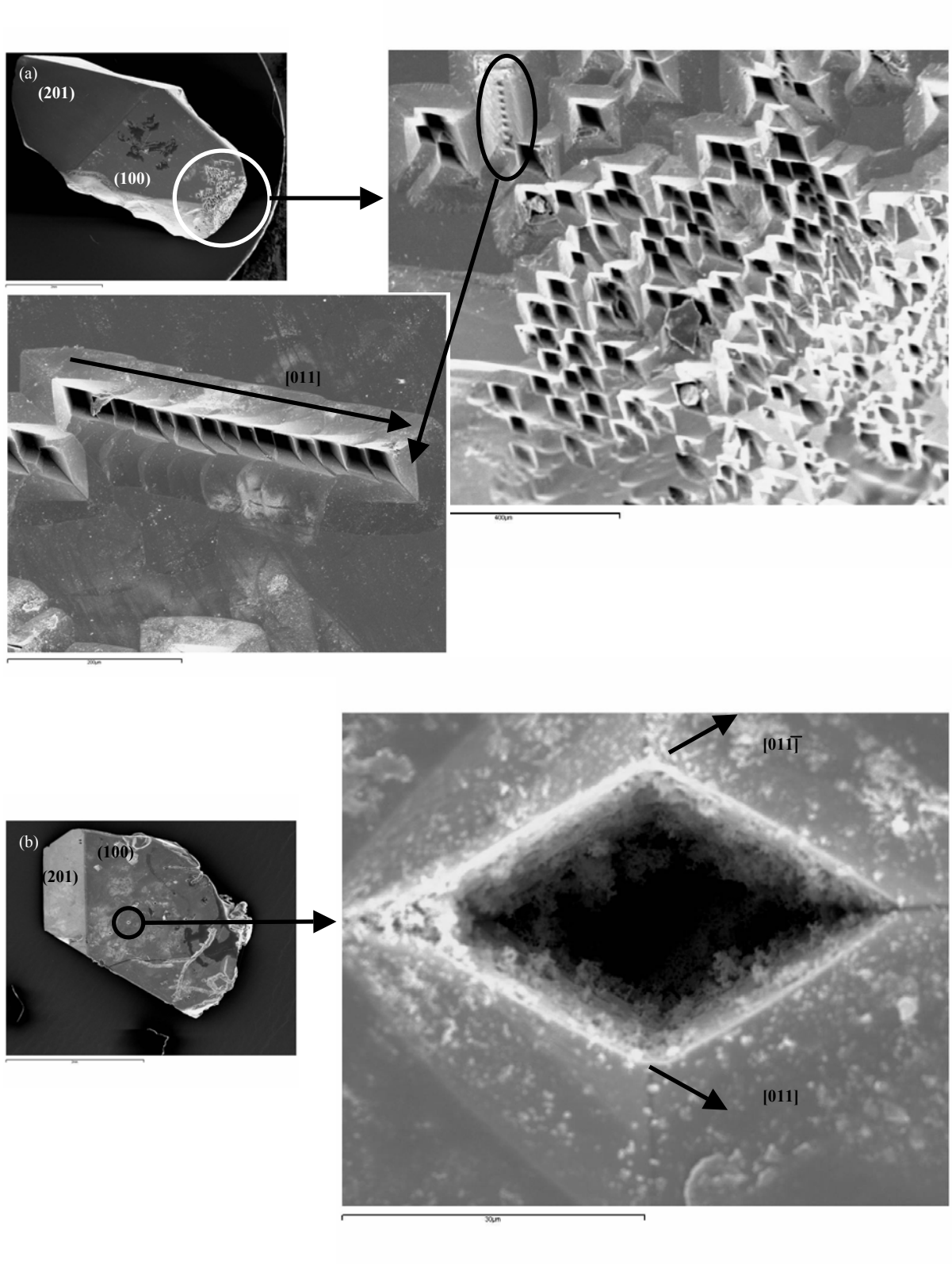

Figure 5.6. *Chemical attack on the {100} faces of (a) RTP crystal and (b) RTP:Nb crystal.*

We obtained a new proof of the different nature of the growth of the {100} and {201} faces in the RTP and RTP:Nb crystals by chemical attacking of these crystals with a mixture of H_2SO_4 (96 %) and HF (40 %) at a volume ratio of 75:25. Figure 5.6 shows the results of this chemical attack on the {100} face of these crystals. Both crystals show rhombohedral etchpits corresponding to dislocations in the area of the crystal with the most defects. These dislocations are aligned along the [011] direction, which is the same direction towards which the edges of the etchpits are oriented. Both crystals have the same behaviour in this face.

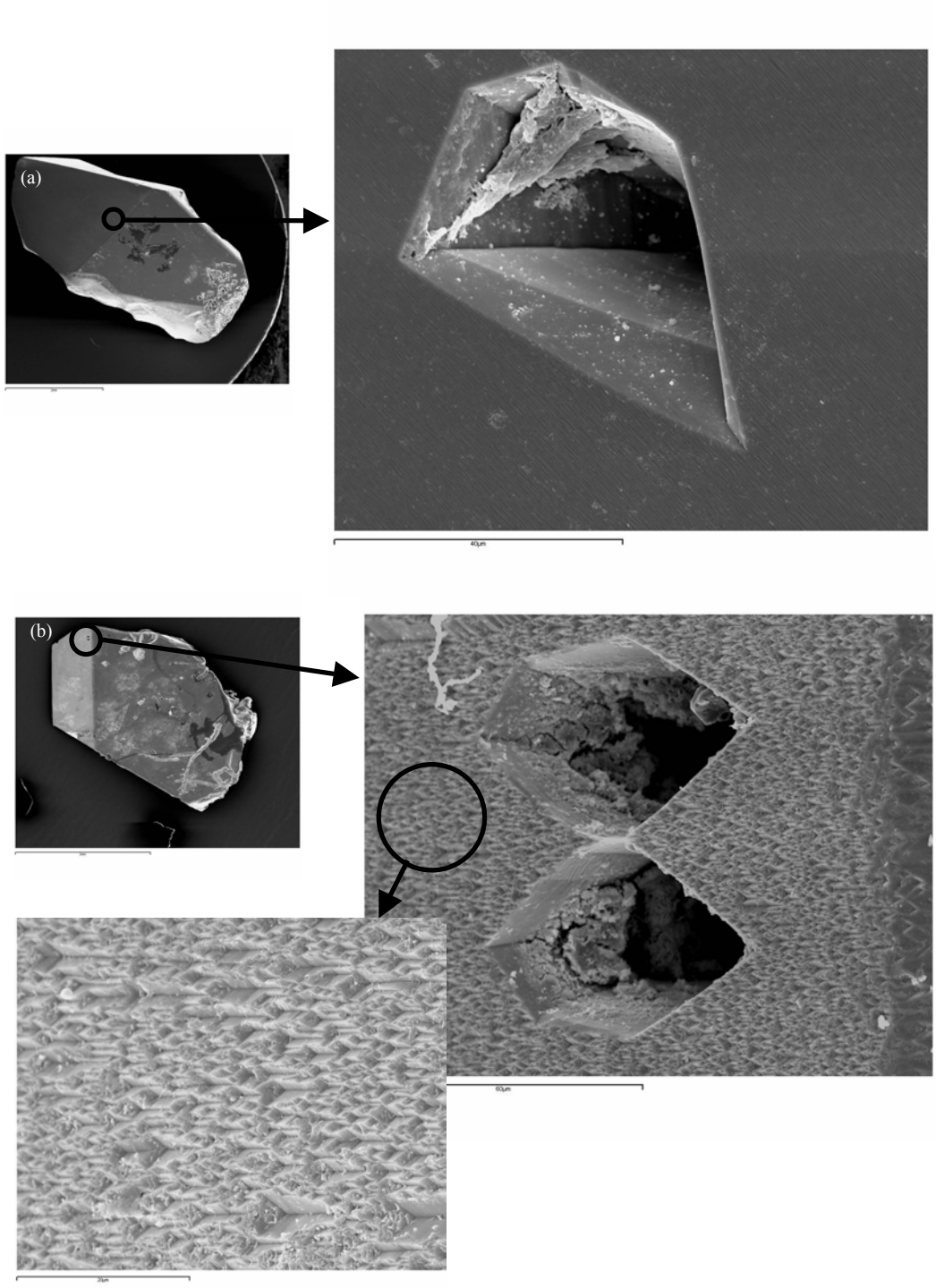

Figure 5.7. *Chemical attack on the {201} face of (a) RTP crystal and (b) RTP:Nb crystal.*

However, a significant change was observed in the chemical attack on the {201} face of these crystals. This face is not attacked in RTP crystals, but it is considerably attacked in RTP:Nb crystals (see Figure 5.7), which reveals the different orientation of the crystallisation units to respect the surface of the face, suggesting a kinked aspect. Then this face will grow faster than the {100} face, and its importance in the last morphology of the crystal will decrease, showing a smaller area.

5.1.3. Crystal growth with a platinum stirrer.

As the solution becomes ever more viscous, problems caused by the formation of inclusion flaws during the advanced stages of the crystal growth process become more evident. In highly viscous solutions, as with the growth solution of RTP and derivative crystals, a drop in temperature leads to a high level of supersaturation in some areas of unstirred growth solutions. In these areas, crystals grow quickly, especially in the direction with the highest growth velocity. With crystals containing Nb, this quick growth accentuates their morphological problems. For these reasons, we developed an acentric crystal growth system comprising a stirrer immersed in the growth solution and two crystal seeds in contact with the solution surface, symmetrically distributed at about 1.5 cm from the rotation axis and 2 cm up the platinum turbine, which acted as a stirrer (see Figure 1 in *paper V*). This system increased the stirring of the solution and favoured the mass transport conditions, thus minimising problems associated with nonhomogeneous supersaturation in these viscous solutions. Stirring the solution also decreased the frequency of spontaneous nucleation during the growth process.

To obtain the most suitable shape for our stirrer, we visually checked the path that the structural units would follow in the growth solution by experimental simulation in a solution containing 90 % glycerine and 10 % water. The viscosity of this solution is around 200 cp at room temperature, which is the one we assumed for our solution at high temperature by comparing it with similar solutions used in the crystal growth of KTP.[185] This solution was placed in a transparent glass crucible with the same dimensions as our Pt crucible. To visually check the path of the structural units in the solution, we used small particles of graphite. Stirrers with several shapes, immersed at various distances in the solution and rotated at different angular velocities were studied. Our results show that the higher the velocity of rotation, the greater the efficiency of the mass transport in the solution. However, the same effect can be obtained by decreasing the velocity of rotation and using a stirrer with a higher number of blades. This is important because if the velocity of rotation is too high, we obtain crystals of the shape shown in Figure 5.8. We then used a platinum stirrer with a high number of blades and rotated at a velocity that did not involve elevating the surface of the solution.

Using this acentric system of crystal growth, we grew crystals of RTP, RTP:W, RTP:Nb, RTP:(Nb,Yb) and RTP:(Nb,Er,W). We obtained a higher quantity of high-quality inclusion-free single

crystals. In these experiments all the crystal seeds used were ***c***-oriented. This is because it has been reported that a seed with a dominant (001) artificial face leads to small capping regions and a low dislocation density in the crystal.[205-206] Figure 5.9 shows some of the crystals we obtained with this acentric crystal growth system.

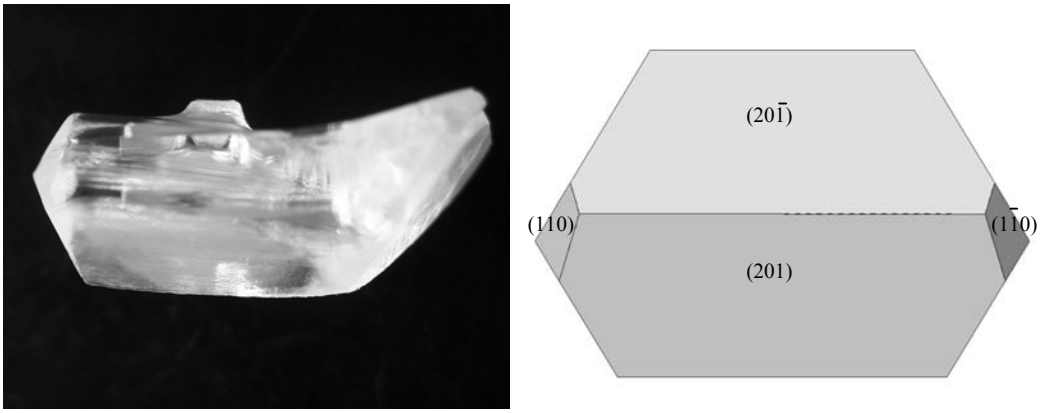

Figure 5.8. *Crystal shape produced in an RTP crystal when the velocity of rotation of the acentric crystal growth system is too high.*

All the features observed in the growth conditions of crystals without additional stirring were also valid in this case. Also, in solutions containing Yb, the temperature of homogenisation of the solution was higher than in the other cases, and the average time of homogenisation was as high as with solutions containing Nb. However, the saturation temperature of crystals containing Yb was always lower than in RTP and RTP:Nb crystals. We found that, in the crystal growth of pure RTP crystals, when the solution was richer in TiO_2, we obtained larger crystals in a smaller cooling interval but fewer high-quality crystals, because as the solution is poorer in P_2O_5 its viscosity is lower. Also the RTP crystals grown in a solution that was poor in TiO_2 were yellowish. This may have been due to some Rb or O vacancies, because the concentration analyses by EPMA found no doping elements in these crystals. In the crystal growth of pure RTP crystals, we also checked the use of RTP:W seeds. Our results indicate that with both, RTP and RTP:W crystal seeds we obtained high-quality crystals. They seem to indicate that the development in the ***b*** and ***c*** directions in RTP:Nb and RTP:(Nb,Yb) crystals became similar, while the development in the ***a*** direction was always lower, as we can see by the size of the crystals in Tables 5.2 and 5.3.

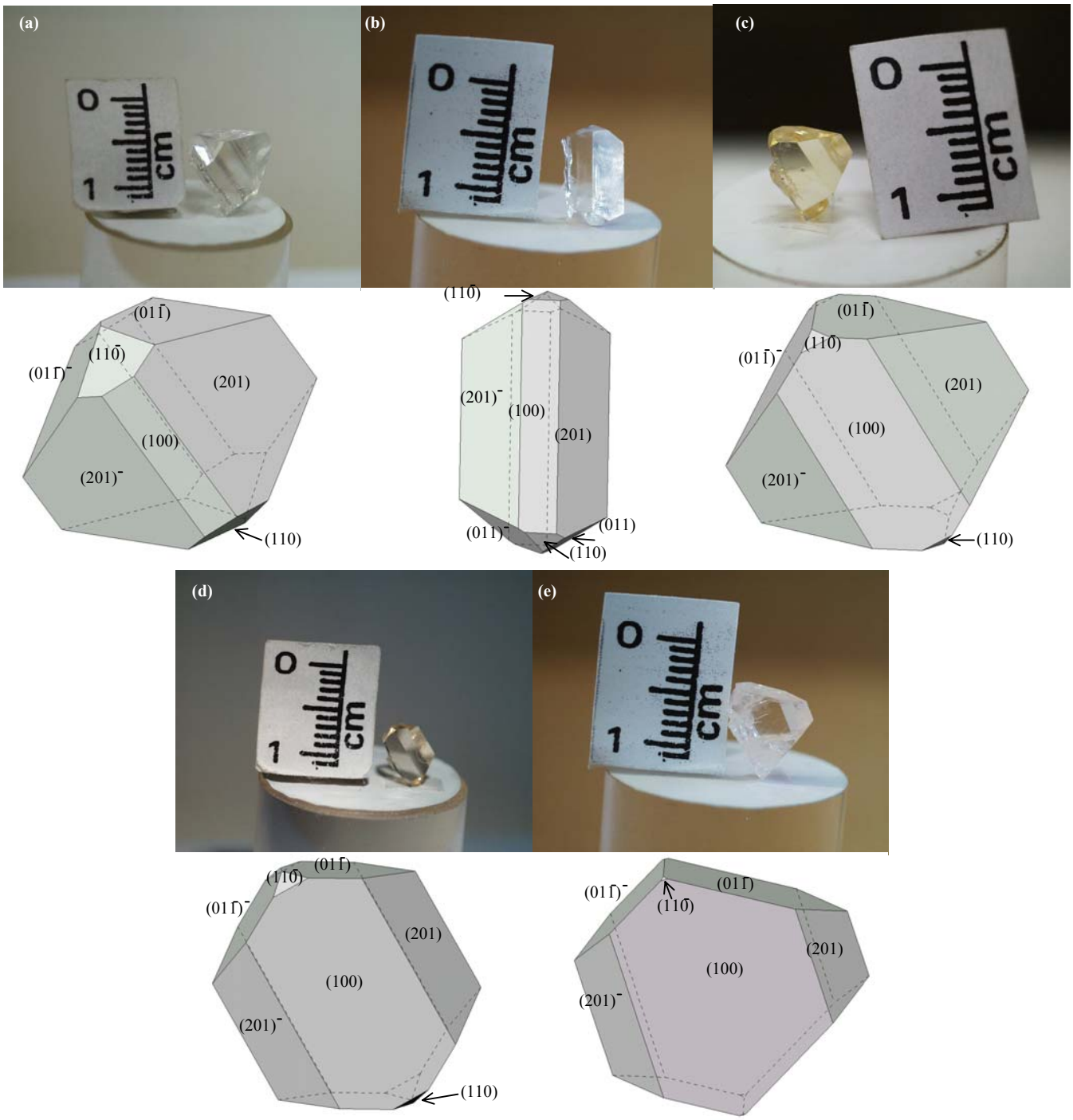

Figure 5.9. *Single crystals of (a) RTP, (b) RTP:W, (c) RTP:Nb, (d) RTP:(Nb,Yb) and (e) RTP:(Nb,Er,W) grown with the acentric crystal growth system.*

In this case we differentiate between the crystal growth experiments performed in cylindrical Pt crucibles of 125 cm^3 (Table 5.2) and conical Pt crucibles of 25 cm^3 (Table 5.3). This is because in the conical crucibles we looked at several parameters such as the efficiency of the crystal growth process and the average supersaturation of the solution (defined in *paper V* and *paper VI*) to evaluate the different conditions of growth. Significant differences were found in these parameters. When Nb_2O_5

was present in the solution, the efficiency of the crystal growth process decreased quickly as the concentration of Nb_2O_5 increased in comparison with the efficiency of the crystal growth of RTP. Also, the crystal growth process was more efficient in solutions with a higher Rb_2O/P_2O_5 ratio under the same growth conditions of temperature gradient, turbine stirring, cooling rate, etc. However, if we increase the cooling interval of the experiment, the number of cracks and flux inclusions increase. It is important to note that whenever Nb and Ln were present in the solution, the crystals were smaller than in the experiments to grow pure RTP crystals with a similar solution composition and the same conditions.

As with the efficiency, average supersaturation of the solution decreases as the concentration of Nb_2O_5 in the solution increases, but no changes where observed when the Rb_2O/P_2O_5 ratio in the composition of the solution changed. This parameter does seem to change in experiments to growth RTP:(Nb,Yb) crystals but we cannot confirm this hypothesis because it is difficult to grow these crystals in crucibles of 25 cm^3 with different concentration of Nb and Yb in the solutions. We also found that for solution compositions in the region in which the saturation temperature is high, the solution climbs high up the crucible walls, and growth device and evaporation are high. These compositions are therefore unsuitable for growing RTP:(Nb,Ln) single crystals.

The temperature of saturation is lower when Nb and Ln are incorporated into the solution than with pure RTP. Also, this T_s was lower when we used the acentric growth system. We can see this if we compare the growth experiments of crystals in solutions containing 20 % of WO_3. This behaviour does not depend on the presence of Nb and Er in the solution. We therefore believe that all solutions used in this Thesis behave in the same way though we do not have enough results to corroborate our opinion.

When we used these small crucibles we also found that if the crystal grows near the blades of the turbine, there are flow inclusions in the lower part of the crystal.

It is difficult to obtain crack- and inclusion-free single crystals for all the different ways of fixing the crystal seeds. In crystals containing Nb, some cracks normally appear in the crystal coming from the seed, which are exacerbated when the concentration of Nb_2O_5 in the solution increases. This problem was not observed in crystals containing only Ln, as we explained in *paper V*. We thought that this problem may have been associated with the mismatch between the cell parameters of RTP and those of RTP:Nb when RTP seeds were used to growth crystals containing Nb. To try to avoid these cracks, we made comparative growth attempts with RTP and RTP:Nb seeds and concluded that cracks appear less often when RTP:Nb seeds are used. At this stage, however, cracks could not be fully avoided, contrary to reports in the literature for KTP doped with Nb.[102] In crystals containing Nb and Ln, we made comparative growth attempts with RTP:Nb seeds and seeds with the same composition as the crystal we wanted to grow. We concluded that, though cracks cannot be fully avoided, they appear less often when the composition of the seed and the crystal we want to growth are the same.

Table 5.2. *Growth data associated with RTP, RTP:Nb and RTP:(Nb,Yb) single crystals grown with the acentric crystal growth system in Pt crucibles of 125 cm^3.*

A	B	C	D	E	F	G	H
42.9-35.1-22.0-0.0-0.0	176	1191	RTP	2.3 K/0.1K·h^{-1} 12 K/0.05 K·h^{-1}	8.8 × 10.3 × 9.0 8.0 × 7.0 × 7.5	1.417	Very good
42.9-35.1-22.0-0.0-0.0	176	1180	RTP	3 K/0.1K·h^{-1} 15.8 K/0.05 K·h^{-1}	10.5 × 10.5 × 9.0 9.0 × 9.5 × 8.5	2.113	Small inclusions and cracks
40.8-27.2-32.0-0.0-0.0	151	1201	RTP	5 K/0.1K·h^{-1} 5 K/0.05 K·h^{-1} 5 K/0.02 K·h^{-1}	7.3 × 12.5 × 6.3 8.0 × 18.5 × 7.2	2.875	Inclusions
40.8-27.2-32.0-0.0-0.0	151	1195	RTP:W	2.5 K/0.1K·h^{-1} 5 K/0.05 K·h^{-1} 7 K/0.02 K·h^{-1}	8.2 × 11.1 × 5.5 10.5 × 15.6 × 7.9	3.378	A small crack
42.9-35.1-21.6-0.4-0.0	180	1193	RTP	3 K/0.1K·h^{-1} 15.4 K/0.05 K·h^{-1}	7.7 × 14.2 × 9.0 6.0 × 14.0 × 9.5	3.889	Cracks and inclusions
42.9-35.1-21.6-0.4-0.0	180	1196	RTP:Nb	3 K/0.1K·h^{-1} 10.5 K/0.05 K·h^{-1}	2.7 × 7.3 × 4.5 3.3 × 7.4 × 6.1	0.495	Very good
42.9-35.1-20.7-1.3-0.0	185	1199	RTP:Nb	3 K/0.1K·h^{-1} 10 K/0.05 K·h^{-1}	3.1 × 3.7 × 4.4 2.5 × 2.8 × 2.8	0.138	Very good
42.9-35.1-20.7-1.3-0.0	185	1195	RTP:Nb	3 K/0.1K·h^{-1} 16.9 K/0.05 K·h^{-1}	4.3 × 8.1 × 7.2 2.1 × 7.4 × 4.8	0.625	Small cracks
42.9-35.1-20.7-1.3-0.0	185	1194	RTP:Nb	5 K/0.1K·h^{-1} 5 K/0.05 K·h^{-1} 9.1 K/0.02 K·h^{-1}	3.0 × 9.2 × 5.9 2.5 × 9.3 × 5.8	0.679	Some inclusions
42.9-35.1-20.2-1.3-0.4	191	1185	RTP:Nb	5 K/0.1K·h^{-1} 5 K/0.05 K·h^{-1} 5 K/0.02 K·h^{-1}	3.6 × 6.3 × 6.6 1.6 × 5.0 × 4.3	0.324	Small inclusions

A: Solution composition (Rb_2O-P_2O_5-TiO_2-Nb_2O_5-Yb_2O_3) (mol %). **B**: Solution weight (g). **C**: T_s (K). **D**: Crystal seed. **E**: Cooling program. **F**: Crystal dimensions in ***a***, ***b*** and ***c*** crystallographic directions, respectively (mm). **G**: Crystal weight (g). **H**: Quality of the crystal.

In these crystals, containing Nb and grown using the acentric crystal growth system, the differences in dimension between the ***a***, ***b***, and ***c*** directions decrease and the crystals become more isometric. However, in all cases the dimension in the ***a*** direction is smaller than the dimensions in the ***b*** and ***c*** directions. This shape makes it difficult to use these crystals in applications, such as SHG, that require a special cut of the sample in the *x*-*y* plane.

Table 5.3. *Growth data associated with RTP, RTP:W, RTP:Nb, RTP:(Nb,Er), RTP:(Nb,Yb) and RTP:(Nb,Er,W) single crystals grown with the acentric crystal growth system in Pt crucibles of 25 cm^3.*

A	B	C	D	E	F	G	H	I	J
40.8-27.2-32.0-0.0-0.0-0.0-0.0	41	1224	RTP:W	6	50	5.9 × 9.2 × 5.4 3.3 × 7.7 × 3.6	0.672	0.27	Very good
42.9-35.1-22.0-0.0-0.0-0.0-0.0	40	1197	RTP			9.8 × 6.6 × 6.2 5.0 × 6.0 × 6.0	0.879		Very good
43.1-31.9-25.0-0.0-0.0-0.0-0.0	40	1215	RTP:W	11.5		5.0 × 6.3 × 4.5 6.9 × 8.9 × 5.9	0.906		Small inclusions
44.2-19.0-16.8-0.0-0.0-0.0-20.0	38	1129	RTP:W	8.5	71	4.7 × 10.0 × 5.6 3.0 × 3.2 × 4.5	0.572		Very good
42.9-35.1-21.6-0.4-0.0-0.0-0.0	41.5	1185	RTP			2.5 × 6.0 × 5.0 4.3 × 7.3 × 6.5	0.475		Small cracks and inclusions
42.9-35.1-21.6-1.3-0.0-0.0-0.0	44	1185	RTP	2	18.2	2.8 × 5.0 × 5.0 1.5 × 4.0 × 3.0	0.163	0.170	Cracks
44.4-29.6-24.7-0.8-0.5-0.0-0.0	26	1164	RTP	1	8.3	1.6 × 1.4 × 1.4 1.6 × 3.0 × 1.4	0.024	0.092	Very good
43.1-31.9-23.7-0.7-0.5-0.0-0.0	39	1194	RTP			2.5 × 5.0 × 5.8 2.4 × 6.2 × 6.7	0.348		Inclusions
43.1-31.9-23.7-0.7-0.5-0.0-0.0	39	1202	RTP			2.7 × 9.9 × 7.6 2.2 × 6.4 × 4.9	0.538		Cracks and inclusions (*)
42.9-35.1-20.9-0.7-0.4-0.0-0.0	29.5	1173	RTP	4	50	2.1 × 5.5 × 5.2 2.2 × 5.0 × 4.5	0.260	0.122	Cracks and inclusions
42.0-28.0-28.5-0.9-0.6-0.0-0.0	28	1193	RTP	1.5	12	2.4 × 2.3 × 2.8 1.9 × 1.9 × 2.1	0.040	0.096	Inclusions
41.0-33.7-23.7-0.7-0.5-0.0-0.0	37	1215	RTP	6.5	59	2.5 × 5.0 × 5.0 2.7 × 4.5 × 4.5	0.237	0.100	Very good
44.2-24.2-16.0-0.5-0.3-0.0-20.0	24	1119	RTP:W			3.0 × 3.5 × 3.8 2.8 × 3.6 × 4.0	0.154		Small cracks and inclusions
40.8-27.2-30.1-0.6-0.0-1.3-0.0	44	1218	RTP:W			3.7 × 13.0 × 7.5	0.640		Inclusions
40.8-27.2-30.4-1.0-0.0-0.6-0.0	44	1215	RTP:W			2.8 × 13.9 × 7.0	0.687		Cracks and inclusions
40.8-27.2-30.1-1.0-0.0-1.0-0.0	43	1204	RTP:W	3.5	29.2	1.8 × 3.7 × 3.7 1.7 × 3.2 × 3.5	0.082	0.056	Cracks

A: Solution composition (Rb_2O-P_2O_5-TiO_2-Nb_2O_5-Er_2O_3-Yb_2O_3-WO_3) (mol %). **B**: Solution weight (g). **C**: T_s (K). **D**: Crystal seed. **E**: ΔT_s. **F**: Efficiency of the process of growth. **G**: Crystal dimensions in ***a***, ***b*** and ***c*** crystallographic directions, respectively (mm). **H**: Crystal weight (g). **I**: Average of supersaturation of the solution (g/K × 100 g solution). **J**: Quality of the crystal. The cooling program was of 12 K at 1 K per day, except in (*), where we applied a cooling program of 25 K/0.1K·h^{-1}.

5.1.4. The change in morphology introduced by thick crystal seeds

To solve the morphological problems of crystals containing Nb we tried to force the growth in the ***a*** direction in crystals containing Nb by using crystal seeds of 5.0 × 1.5 × 5.0 mm in the ***a*** × ***b*** × ***c*** directions. With this kind of crystal seeds we grew RTP:Nb and RTP:(Nb,Yb) crystals on RTP:Nb and RTP:(Nb,Yb) seeds (see Table 5.4). In this way we obtained crystals of RTP doped with Nb and co-doped with Nb and Yb of typical dimensions of 5 × 5 × 5 mm in the ***a*** × ***b*** × ***c*** directions. Figure 5.10

shows one of the crystals obtained with these thick crystal seeds. We obtained some high-quality crystals without cracks using solutions containing only Nb, but when we introduced Yb to the solution, more cracks appeared, due to internal stresses in the crystals. Normally they were not present when we pulled the crystals out of the furnace, but when we cut the crystal seed, many cracks appeared. As Table 5.4 shows, the temperature of saturation was lowest in crystals containing Nb and Yb, followed by those containing only Nb. The temperature of saturation was the highest for pure RTP crystals when the experiments were performed in solutions with a similar composition and the same conditions of growth were maintained. Also, although the crystals were larger than when crystal seeds of 1.5 × 1.5 × 5.0 mm in the ***a*** × ***b*** × ***c*** directions were used, size and weight were still lower than with pure RTP crystals grown in the same conditions.

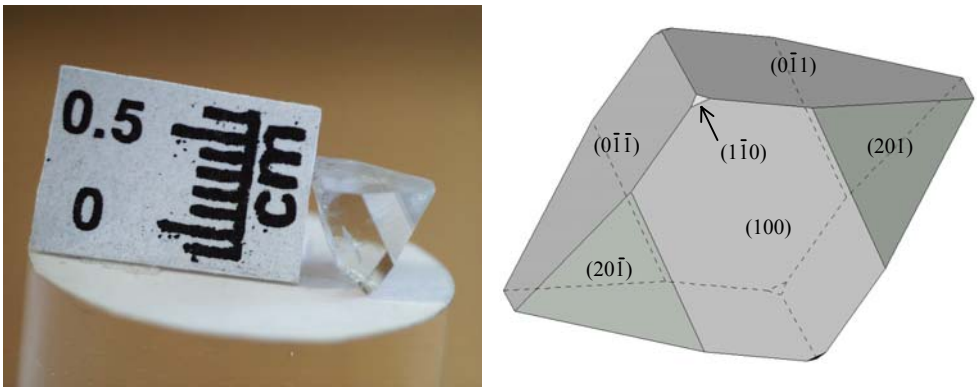

Figure 5.10. *Single crystal of RTP:Nb grown with the acentric crystal growth system using thick crystal seeds in the* ***a*** *direction.*

Table 5.4. *Growth data associated with RTP:Nb and RTP:(Nb,Yb) single crystals grown with the acentric crystal growth system using thick crystal seeds in the* ***a*** *direction.*

A	B	C	D	E	F	G	H
40.8-27.2-31.0-1.0-0.0	158	1192	RTP:Nb	2.5 K/0.1K·h^{-1} 5 K/0.05 K·h^{-1} 7.5 K/0.02 K·h^{-1}	6.2 × 6.9 × 7.8 6.7 × 5.7 × 6.7	1.977	Very good
40.8-27.2-31.0-1.0-0.0	158	1191	RTP:Nb	2.5 K/0.1K·h^{-1} 5 K/0.05 K·h^{-1} 6.6 K/0.02 K·h^{-1}	6.5 × 6.1 × 7.4 6.3 × 6.6 × 7.6	1.105	Some inclusions
40.8-27.2-30.4-1.0-0.6	164	1172	RTP:Nb	2.5 K/0.1K·h^{-1} 5 K/0.05 K·h^{-1} 7.5 K/0.02 K·h^{-1}	7.8 × 6.2 × 7.3 6.5 × 6.6 × 6.5	1.287	Cracks and inclusions
40.8-27.2-30.4-1.0-0.6	164	1176	RTP:(Nb,Yb)	2.5 K/0.1K·h^{-1} 2.5 K/0.05 K·h^{-1} 7.7 K/0.02 K·h^{-1}	6.3 × 4.8 × 4.5 4.5 × 5.0 × 6.3	1.513	Cracks

A: Solution composition (Rb_2O-P_2O_5-TiO_2-Nb_2O_5--Yb_2O_3) (mol %). **B**: Solution weight (g). **C**: T_s (K). **D**: Crystal seed. **E**: Cooling program. **F**: Crystal dimensions in ***a***, ***b*** and ***c*** crystallographic directions, respectively (mm). **G**: Crystal weight (g). **H**: Quality of the crystal.

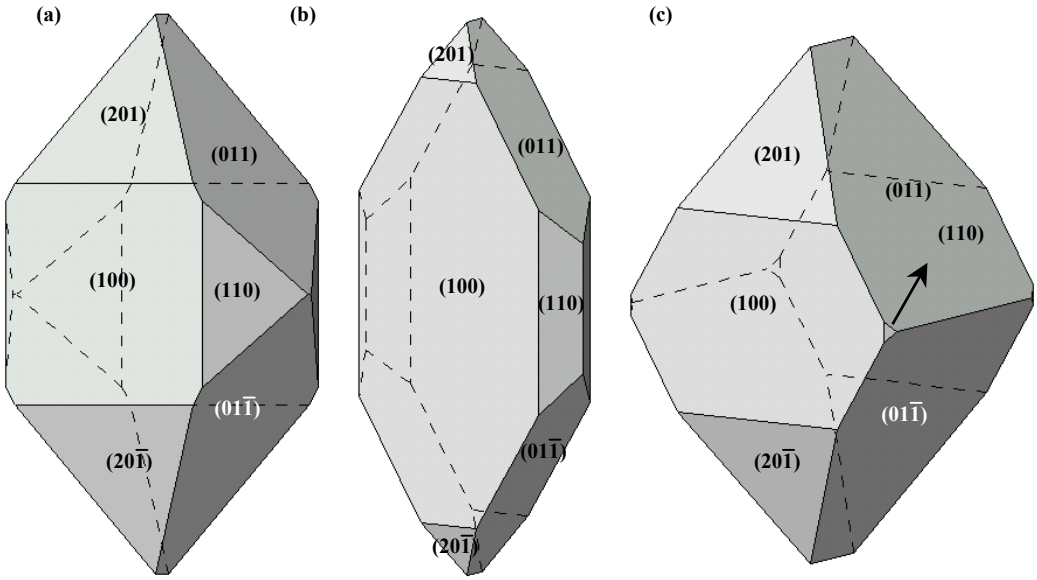

Figure 5.11. *Morphology of (a) RTP crystal, (b) RTP:Nb crystal grown using a thin crystal seed in the* ***a*** *direction and (c) RTP:Nb crystal grown using a thick crystal seed in the* ***a*** *direction.*

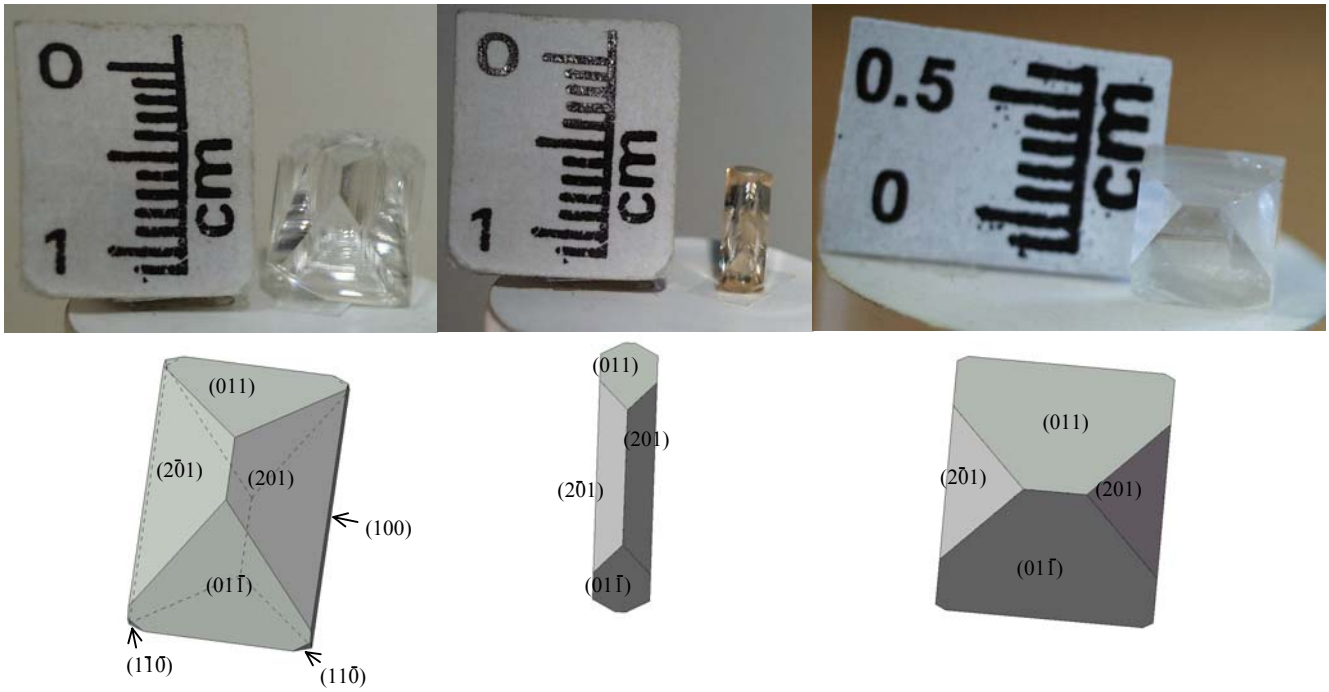

Figure 5.12. *(a) RTP crystal, (b) RTP:Nb crystal grown using a thin crystal seed in the* ***a*** *direction and (c) RTP:Nb crystal grown using a thick crystal seed in the* ***a*** *direction.*

The morphology of the crystals grown using these thick crystal seeds was different from that of RTP and RTP:Nb crystals (see Figure 5.11) by comparison with the morphology of RTP and RTP:Nb crystals grown using thinner crystal seeds in the ***a*** direction. The forced crystal growth in the ***a*** direction causes the {110} form to disappear. Also, the {011} and the $\{01\bar{1}\}$ forms are more important

than in RTP crystals containing Nb grown in thin crystal seeds in ***a*** direction. All these aspects are also shown in Figure 5.12, which compares crystals of RTP:Nb grown with thick and thin crystal seeds in the ***a*** direction. This new morphology provides a large useful area of crystal in the *x*-*y* plane with benefits for later applications, because samples for SHG and self-frequency doubling applications must be cut in this plane.

5.2. Concentration analyses.

The dopant concentration in the crystals was analysed by Electron Probe Microanalyses (EPMA). From these results and the concentrations of these ions in the solutions, we calculated the distribution coefficients for each doping ion (defined in *papers II, IV, V and VI*). Our results are given in Table 5.5.

Table 5.5. *Distribution coefficients of Er, Yb, Nb and W in RTP crystals.*

A	B	C	D	E	F	G
43.9-23.6-22.5-0.0-0.0-0.0-10.0	Conical				Not measurable	
44.2-19.0-16.8-0.0-0.0-0.0-20.0	Conical				0.009	$RbTi_{0.995}W_{0.005}OPO_4$
43.7-23.5-12.8-0.0-0.0-0.0-20.0	Conical				0.006	$RbTi_{0.996}W_{0.004}OPO_4$
42.9-35.1-21.6-0.4-0.0-0.0-0.0	Conical	0.56				$RbTi_{0.978}Nb_{0.022}OPO_4$
42.9-35.1-21.6-1.3-0.0-0.0-0.0	Conical	0.49				$RbTi_{0.941}Nb_{0.059}OPO_4$
40.8-27.2-31.0-1.0-0.0-0.0-0.0	Cylindrical	0.56				$RbTi_{0.966}Nb_{0.034}OPO_4$
44.4-29.6-24.7-0.8-0.5-0.0-0.0	Conical	0.26	0.06			$RbTi_{0.983}Nb_{0.015}Er_{0002}OPO_4$
43.1-31.9-23.7-0.7-0.5-0.0-0.0	Conical	0.62	0.08			$RbTi_{0.960}Nb_{0.037}Er_{0.003}OPO_4$
42.9-35.1-20.9-0.7-0.4-0.0-0.0	Conical	0.57	0.04			$RbTi_{0.966}Nb_{0.032}Er_{0.002}OPO_4$
42.0-28.0-27.9-1.2-0.9-0.0-0.0	Cylindrical	0.56	0.16			$RbTi_{0.938}Nb_{0.053}Er_{0.009}OPO_4$
42.0-28.0-27.9-1.2-0.9-0.0-0.0	Conical	0.52	0.21			$RbTi_{0.949}Nb_{0.039}Er_{0.012}OPO_4$
42.0-28.0-28.5-0.9-0.6-0.0-0.0	Conical	0.37	0.14			$RbTi_{0.974}Nb_{0.021}Er_{0.005}OPO_4$
42.0-28.0-28.5-0.6-0.9-0.0-0.0	Cylindrical	0.65	0.12			$RbTi_{0.967}Nb_{0.026}Er_{0.007}OPO_4$
41.2-33.7-23.7-0.7-0.5-0.0-0.0	Conical	0.62	0.04			$RbTi_{0.963}Nb_{0.036}Er_{0.001}OPO_4$
44.2-19.0-16.0-0.5-0.3-0.0-20.0	Conical	0.63	0.24		0.01	$RbTi_{0.951}Nb_{0.038}Er_{0.098}W_{0.007}OPO_4$
42.9-35.1-20.2-1.3-0.0-0.4-0.0	Cylindrical	0.63		0.35		$RbTi_{0.910}Nb_{0.076}Yb_{0.014}OPO_4$
42.0-28.0-28.2-0.9-0.0-0.9-0.0	Conical	0.77		0.37		$RbTi_{0.934}Nb_{0.044}Yb_{0.022}OPO_4$
40.8-27.2-30.1-0.6-0.0-1.3-0.0	Conical	0.75		0.21		$RbTi_{0.953}Nb_{0.030}Yb_{0.017}OPO_4$
40.8-27.2-30.4-1.0-0.0-0.6-0.0	Conical	0.73		0.36		$RbTi_{0.942}Nb_{0.044}Yb_{0.014}OPO_4$
40.8-27.2-30.4-1.0-0.0-0.6-0.0	Cylindrical	0.74		0.52		$RbTi_{0.934}Nb_{0.045}Yb_{0.021}OPO_4$
40.8-27.2-30.1-1.0-0.0-1.0-0.0	Conical	0.60		0.50		$RbTi_{0.934}Nb_{0.036}Yb_{0.030}OPO_4$

A: Solution composition (Rb_2O-P_2O_5-TiO_2-Nb_2O_5-Er_2O_3-Yb_2O_3-WO_3) (mol %). **B**: Crucible shape. **C**: K_{Nb}. **D**: K_{Er}. **E**: K_{Yb}. **F**: K_W. **G**: Stoichiometry.

The distribution coefficients of the Ln in these crystals were slightly lower than when we calculated them with crystals grown on a Pt rod, without seeds, when we studied the corresponding crystallisation region (see Chapter 3). This may be due to the additional stirring of the solution during the growth experiments, which improves homogeneity and mass transport efficiency in the solution, and to the different rate of cooling and, therefore, to the different velocity of growth. There are several differences between doping with Er^{3+} and doping with Yb^{3+}. These depend on whether the experiments were performed in small conical crucibles or in larger cylindrical crucibles. Although there were no differences in the distribution coefficients of Er, the distribution coefficient of Yb was significantly higher in the experiments performed in cylindrical crucibles. However, the crystals of RTP:(Nb,Yb) obtained in small conical crucibles were of such low quality that the results were not conclusive. As we found when we studied the crystallisation regions of RTP crystals codoped with Nb and Ln ions, for solutions containing a similar content in Er, the distribution coefficient of this ion increased, for the range of concentrations studied in these crystal growth experiments, as the concentration of Nb in the solution increased. However, for solutions with a similar concentration of Yb, the distribution coefficient of this ion practically did not change as the concentration of Nb in the solution increased. In RTP:(Nb,Er) experiments, the distribution coefficient of Er was lower for crystals grown in solutions with a higher Rb_2O/P_2O_5 ratio. The distribution coefficients increased considerably in solutions containing WO_3. In fact they were the highest obtained in this Thesis. We did not study these crystals, however, because we tried to understand the effect of Nb and lanthanide ions in this matrix so we only characterised crystals grown in self-flux. Finally, except in the crystal growth of RTP:(Nb,Er,W) single crystals, the distribution coefficient of Yb was always higher than that of Er. This was because the smaller ionic radius of Yb^{3+} in an octahedrical environment makes it more similar to that of Ti^{4+} in the same environment (see Chapter 3).

The maximum Ln concentrations achieved in these crystals were $[Yb^{3+}] = 1.96 \times 10^{20}$ atoms·cm^{-3} for RTP:(Nb,Yb) and $[Er^{3+}] = 0.65 \times 10^{20}$ atoms·cm^{-3} for RTP:(Nb,Er). This Er concentration was one order of magnitude larger than that previously obtained in RTP grown without Nb_2O_5 (0.05×10^{20} ions·cm^{-3}) and 36 times higher than that obtained in KTP:Er samples (see *paper I*). The Yb concentration, the highest ever obtained in a bulk crystal of the family of KTP, was also one order of magnitude higher than that previous obtained in KTA.[207]

The distribution coefficient of Nb decreased when the concentration of Nb_2O_5 in the solution increased. We also observed that this distribution coefficient decreased when the concentration of Ln in the solution increased. This may be due to saturation. In all cases the distribution coefficient of Nb was higher than that of Ln. This effect, based on the ionic radii of Nb^{5+} and Ln^{3+} and their similarity to the ionic radius of Ti^{4+}, is explained in Chapter 3. Finally, in RTP:(Nb,Er) experiments, the distribution

coefficient of Nb was higher for crystals grown in solutions containing a higher Rb_2O/P_2O_5 concentration ratio. This may be due to the different viscosities of the solutions (see Chapter 3).

The distribution coefficient of W is higher when the solution is richer in Rb_2O and TiO_2 and poorer in P_2O_5. It was also slightly higher when Nb_2O_5 and Er_2O_3 are present in the solution. This is interesting because any effects that the incorporation of W in the crystals can have on the properties of RTP crystals grown in solutions containing WO_3, will be maintained, but will not increase in RTP:(Nb,Ln) crystals grown in solutions containing WO_3.

The concentrations of the doping ions are not homogeneous along the crystal. Figure 2 in *paper X* shows how the distribution concentration of Yb and Nb changes along the three crystallographic directions of the crystal. Clearly, the closer to the crystal seed, the lower the concentration of both Yb and Nb. This was because the distribution coefficients of these ions were less than one. Therefore, as the crystal grows, the solution gets richer in Nb and Yb and the concentration of these ions in the crystals may increase.

Initial Page **Table of Contents**